Deep glacial troughs and stabilizing ridges unveiled beneath the margins of the Antarctic ice sheet

Mathieu Morlighem [1]*, Eric Rignot [1,2], Tobias Binder[3], Donald Blankenship[4], Reinhard Drews [3,5], Graeme Eagles [3], Olaf Eisen [3,6], Fausto Ferraccioli[7], René Forsberg[8], Peter Fretwell[7], Vikram Goel [9], Jamin S. Greenbaum [4], Hilmar Gudmundsson [10], Jingxue Guo[11], Veit Helm[3], Coen Hofstede[3], Ian Howat[12], Angelika Humbert [3,6], Wilfried Jokat [3], Nanna B. Karlsson [3,13], Won Sang Lee [14], Kenichi Matsuoka [15], Romain Millan[1], Jeremie Mouginot [1,16], John Paden[17], Frank Pattyn [18], Jason Roberts [19,20,21], Sebastian Rosier[10], Antonia Ruppel[22], Helene Seroussi [2], Emma C. Smith [3], Daniel Steinhage [3], Bo Sun[11], Michiel R. van den Broeke [23], Tas D. van Ommen[19,20,21], Melchior van Wessem [23] and Duncan A. Young [4]

The Antarctic ice sheet has been losing mass over past decades through the accelerated flow of its glaciers, conditioned by ocean temperature and bed topography. Glaciers retreating along retrograde slopes (that is, the bed elevation drops in the inland direction) are potentially unstable, while subglacial ridges slow down the glacial retreat. Despite major advances in the mapping of subglacial bed topography, significant sectors of Antarctica remain poorly resolved and critical spatial details are missing. Here we present a novel, high-resolution and physically based description of Antarctic bed topography using mass conservation. Our results reveal previously unknown basal features with major implications for glacier response to climate change. For example, glaciers flowing across the Transantarctic Mountains are protected by broad, stabilizing ridges. Conversely, in the marine basin of Wilkes Land, East Antarctica, we find retrograde slopes along Ninnis and Denman glaciers, with stabilizing slopes beneath Moscow University, Totten and Lambert glacier system, despite corrections in bed elevation of up to 1 km for the latter. This transformative description of bed topography redefines the high- and lower-risk sectors for rapid sea level rise from Antarctica; it will also significantly impact model projections of sea level rise from Antarctica in the coming centuries.

Subglacial bed topography has been measured most efficiently using airborne radio-echo sounding[1]. This technique provides bed elevation measurements directly beneath the aircraft path, but, despite numerous campaigns, major data gaps remain between flight lines and especially across deep glaciers. As a result, there are vast sectors of Antarctica with no data[2]: 85% of Antarctica's surface area does not have any measurement of bed topography within a 1 km radius, and 50% of the ice sheet is more than 5 km from any measurement. The region inland of Princess Elizabeth Land, North of Dome Argus, has an area of more than 90,000 km[2] with no measurement. Major data gaps exist east, west and south of Dome Fuji and west of the Transantarctic Mountains. More importantly, we have no deep sounding near the grounding lines (that is, at the junction with the ocean) of

major glaciers such as Denman Glacier in East Antarctica or the Lambert system.

Bed elevation is difficult to sound for logistical and technical reasons. Radar sounding systems fail to probe deep subglacial troughs because steep valley walls yield side reflections that mask the bed echoes[3,4] and the rough, broken-up glacier surface generates significant radar clutter. Unfortunately, these areas, although small in total area compared to the rest of the continent, are critical to characterize because they control most of the ice discharge from Antarctica. The latest Antarctic-wide bed topography dataset[5], Bedmap2, was a major improvement over previous datasets, but many sectors were still undersampled, especially the glacier troughs. A major limitation of prior approaches was the sole reliance on ice thickness data combined with simple interpolation techniques, such as Kriging or

[1]Department of Earth System Science, University of California, Irvine, CA, USA. [2]Jet Propulsion Laboratory, California Institute of Technology, Pasadena, CA, USA. [3]Alfred Wegener Institute Helmholtz Centre for Polar and Marine Research, Bremerhaven, Germany. [4]Jackson School of Geosciences, UT Austin, Austin, TX, USA. [5]Department of Geosciences, University of Tübingen, Tübingen, Germany. [6]University of Bremen, Bremen, Germany. [7]British Antarctic Survey, Cambridge, UK. [8]Technical University of Denmark, Kongens Lyngby, Denmark. [9]National Centre for Polar and Ocean Research, Vasco, Goa, India. [10]Northumbria University, Newcastle upon Tyne, UK. [11]Polar Research Institute of China, Shanghai, China. [12]School of Earth Sciences, Ohio State University, Columbus, OH, USA. [13]Geological Survey of Denmark and Greenland, Copenhagen, Denmark. [14]Korea Polar Research Institute, Incheon, South Korea. [15]Norwegian Polar Institute, Tromsø, Norway. [16]Institut des Géosciences de l'Environnement, CNRS, Université Grenoble Alpes, Grenoble, France. [17]Center for Remote Sensing of Ice Sheets, University of Kansas, Lawrence, KS, USA. [18]Université libre de Bruxelles, Brussels, Belgium. [19]Australian Antarctic Division, Kingston, Tasmania, Australia. [20]Antarctic Climate & Ecosystems Cooperative Research Centre, Tasmania, Australia. [21]Institute for Marine and Antarctic Studies, University of Tasmania, Hobart, Tasmania, Australia. [22]Federal Institute for Geosciences and Natural Resources, Hanover, Germany. [23]Institute for Marine and Atmospheric Research, Utrecht University, Utrecht, Netherlands. *e-mail: Mathieu.Morlighem@uci.edu
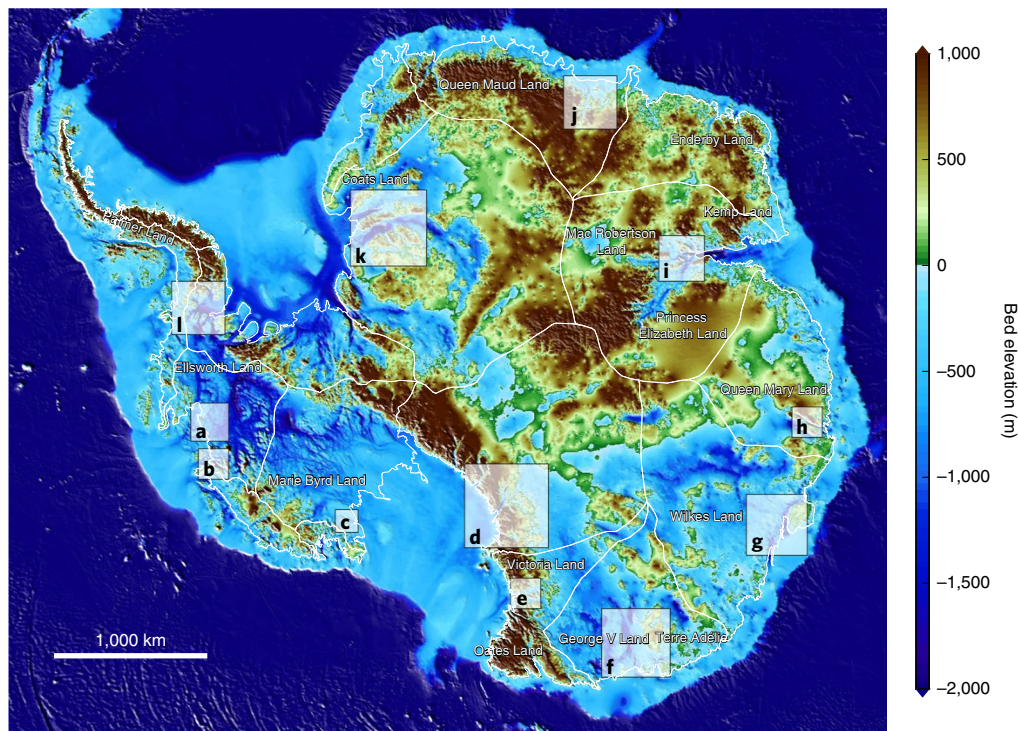
Fig. 1 | Bed elevation of the Antarctic ice sheet colour coded between −2,000 and 1,000 m above sea level. The white lines delineate the basins[15] from the ice sheet mass balance inter-comparison exercise (IMBIE). Regions marked **a**–**l** are explored in Fig. 2.

thin plate splines. These approaches are highly sensitive to measurement density, resulting in ice thickness errors of several hundreds of metres to 1 km in places with few to no observations, as a result of uncontrolled extrapolation. At the grounding line, it is essential to obtain a seamless transition in ice thickness and bed topography because glacier dynamics is particularly sensitive to both properties there. The level of detail required by ice sheet numerical models is typically about one ice thickness, or at least[6] 1 km. It is at that length scale that ridges and sinks in bed topography affect glacier dynamics. The current uncertainty and lack of small-scale detail in existing bed topography profoundly limits our ability to understand current changes in glacier flow and project ice sheet evolution over the coming decades.

Mapping bed topography using mass conservation

To overcome these difficulties, we apply a mass conservation (MC) method[7]. A chief advantage of MC is that it makes use of a fundamental physical law—the conservation of mass—to fill data gaps. The output product is fully compatible with numerical models because mass is conserved in the output product[8]. Second, MC employs corrections for surface mass balance and temporal changes in ice thickness to refine the calculation of ice thickness. The resolution of the data product is no longer defined by the spacing of ice thickness data from radio-echo sounding but by the spatial resolution of the ice surface velocity, which is typically on the order of a few hundred metres for satellite-based datasets. However, the precision of the product is affected by the spacing between ice thickness measurements (which are used to constrain the calculation) and by uncertainties and errors in the ice velocity and the surface mass balance. This methodology has been successfully applied in Greenland to transform our knowledge of bed topography and in turn our understanding of glacier dynamics, ocean circulation, ocean heat transfer, calving dynamics and mechanisms of retreat[9,10]. Applying the same methodology to Antarctica presents a number of

additional challenges due to the sheer size of the continent and the limited density of ice thickness data compared to Greenland.

In this study, we employ ice thickness data from 19 different research institutes, covering more than 1.5 million line kilometres over the time period 1967 to present. We use gravity-derived inversion for ice shelf bathymetry from Operation IceBridge and other projects in a few sectors, complemented by seismic data where available. We use ice flow velocity from satellite interferometry[11,12], surface mass balance from a regional atmospheric climate model[13] and the surface topography from the Reference Elevation Model of Antarctica[14]. The grid size of the output product is 500 m. The spatial domain is divided into a number of fast-flowing areas where we apply MC, and slower moving areas where we use a streamline diffusion method as an alternative to Kriging (see Supplementary Information). Overall, we revise the bed topography over more than 50% of the ice sheet flowing faster than 50 m per year, where MC is most accurate, and cover 71% of the ice discharge from the continent. The results are accompanied by an error map and a source mask (see Supplementary Information), which are needed by modellers and to assist future surveys. The nominal vertical accuracy of MC is 30–60 m but local errors may exceed 100 m in poorly constrained regions. On floating ice, we rely on hydrostatic equilibrium with a firn densification model that is calibrated with all available ice shelf thickness data. This latter approach has the advantage of ensuring continuity in ice thickness across the grounding line.

The new bed compilation is named BedMachine Antarctica (Fig. 1), because the product is regularly updated with new data. At a large scale, the shape of the bed beneath Antarctica is not fundamentally different from that in Bedmap2. We calculate a sea level equivalent (SLE) of 57.9 ± 0.9 m for the Antarctic Ice Sheet (Supplementary Table 3), which is close to the Bedmap2 estimate of 58.3 m. Most differences appear at the smaller scale, yet these local differences have a profound impact on glacier evolution and, in turn, on ice sheet mass balance. As an example, we find that local bed slopes are
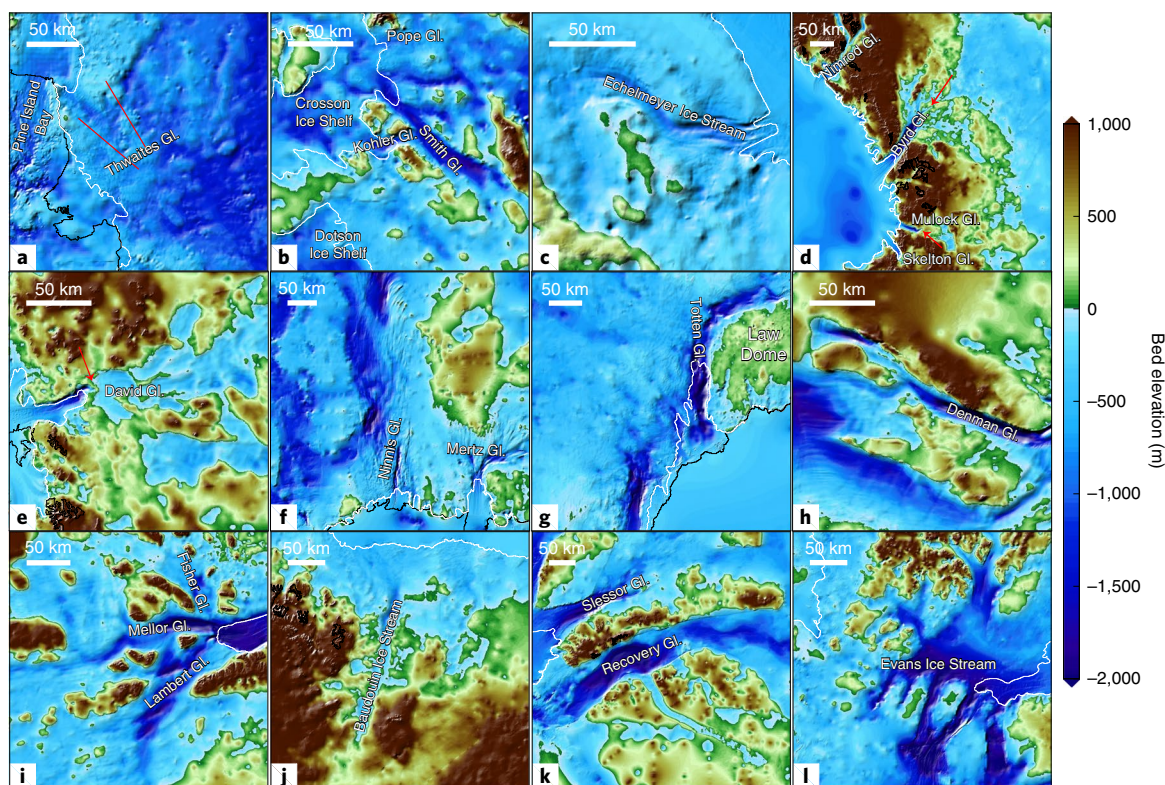
Fig. 2 | Detailed bed topography of Antarctic outlet glaciers. a–l, Bed elevation of Thwaites (**a**) and Kohler, Smith and Pope (**b**) glaciers, Shirase coast (**c**), Byrd and Mulock glaciers (**d**), David (**e**) and Ninnis and Mertz (**f**) glaciers, Moscow University Ice Shelf and Totten glacier (**g**), Denman (**h**) and Lambert (**i**) glaciers, Roi Baudouin Ice Shelf (**j**), Recovery (**k**) and Evans (**l**) Ice Streams, colour coded between −2,000 m and 1,000 m above sea level. The black lines show the ice extent and the white lines the grounding lines. Gl., Glacier.

steeper over 62% of the mapped area when using MC compared to Bedmap2 (Supplementary Fig. 59). In addition, MC captures high-resolution details where Kriging produces a smooth bed topography. The spatial details of the connectivity of individual basins with deep channels and the ocean are revised significantly, which is critical for ice sheet modelling.

New details along coastal margins

In the most rapidly changing sector of Antarctica, the Amundsen Sea Embayment (ASE) (Fig. 2a,b and Supplementary Figs. 6–9), we find that the bed of Thwaites Glacier (65 cm SLE, 118.4 Gt per year discharge[15]) has a granular texture, with no well-defined troughs, which is indicative of a hard, crystalline bedrock[16]. Asperities and bed ridges in the proximity of the grounding zone were, for a large part, missing in previous datasets, but are now found to be in excellent agreement with the observed pattern of retreat[17]. We do not find major bumps in bed topography upstream of the current grounding line that could stop the grounding line retreat, except for two prominent ridges ~35 and 50 km upstream (red lines, Fig. 2a). Ice sheet numerical models indicate that once the glacier retreats past the second ridge, the retreat of Thwaites Glacier would become unstoppable[18–20].

East of Thwaites, the bed topography of Pine Island Glacier at the grounding line (51 cm SLE, 122.6 Gt per year discharge) is 200 m deeper than in Bedmap2 because of erroneous identification of bottom crevasses as the bed[17]. The older Bedmap2 product, still widely used by the modelling community, yields model simulations with limited grounding line retreat or even grounding line advance, both of which contradict observations[21]. Nearby, the bed of Kohler Glacier (Fig. 2b) shows a topographically controlled ice flow, typical of selective linear erosion[22,23], with a significant portion of retrograde slope. The bed of the glaciers between Pope and Smith glaciers is more

continuous than in Bedmap2 and does not include a ridge across the grounding lines (Supplementary Fig. 9), which was an artefact of the gridding method in Bedmap2. The trough of Smith Glacier is one of the deepest and longest in West Antarctica, reaching 2,500 m below sea level, with retrograde slopes where the grounding line is retreating at record rates[17] of 2–2.5 km per year. Along the Shirase coast, West Antarctica (Fig. 2c), we find a previously unknown 100 km-long, 15 km-wide, 1 km-deep valley beneath Echelmeyer Ice Stream that is not resolved in previous maps (Supplementary Fig. 16).

Along the Transantarctic Mountains, we find deeper valleys beneath the outlet glaciers than in Bedmap2 (Fig. 2d). Nimrod, Byrd and Mulock glaciers have a smaller ice discharge than Pine Island and Thwaites Glacier, but have a sea level potential one order of magnitude greater due to their extensive catchments on the East Antarctic plateau. The glaciers flow along narrow submarine valleys, more than 3,000 m below sea level for Byrd Glacier. These deeply incised troughs have been challenging to resolve for radar sounding for decades, as illustrated in Fig. 3b,c, which explains errors >1 km in some places in previous mapping (Fig. 3). In all cases, however, we find that the bed elevation rises rapidly above sea level within a few tens of kilometres of the present-day grounding lines. Byrd Glacier has a prominent subglacial ridge across the Transantarctic Mountains that will provide a strong anchor point for its grounding line. David Glacier, further west (Figs. 2e and 3d), is currently held by a major ridge above the cauldron area that had not been previously resolved (Supplementary Fig. 21). On the eastern side of David Glacier, we find a 2 km-deep, 10 km-wide trough that ends with an ice fall into the Drygalski Ice Tongue. The ice thickness of the ice tongue at the grounding line exceeds 2,500 m, which explains its remarkable stability and exceptional (70 km) extension out to sea, and a 10 km-wide ridge, 100 m above sea level, a few kilometres
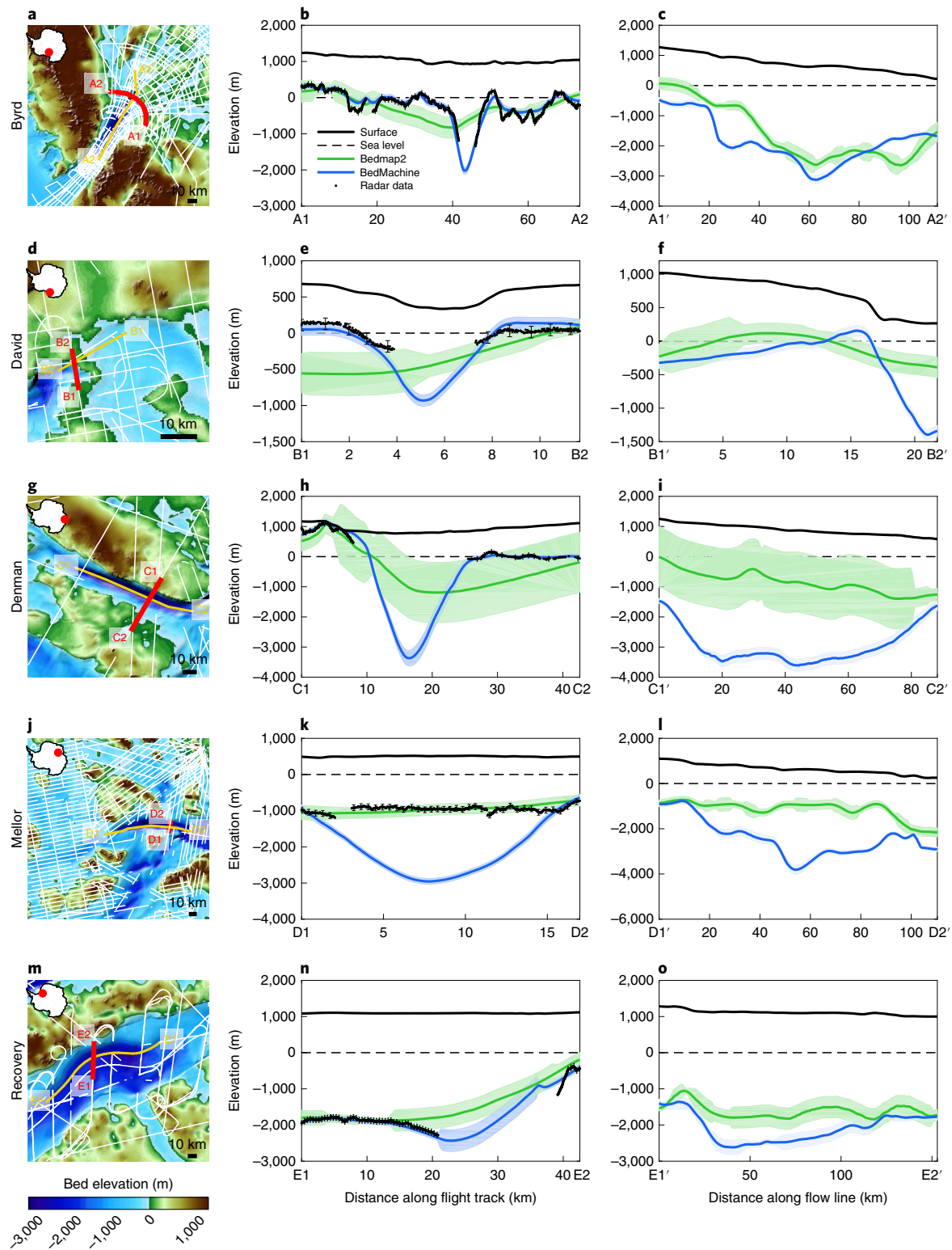
Fig. 3 | Comparison with previous datasets and radar data. a,d,g,j,m, Bed elevations of Byrd (**a**), David (**d**), Denman (**g**), Mellor (**j**) and Recovery (**m**) glaciers, colour coded between −3,000 m and 1,500 m above sea level, with radar profiles shown as white lines where bed reflections were detected. The yellow and red lines (for example, A1–A2 and A1'–A2' in **a**, and so on) show the locations where the profiles in the middle (**b,e,h,k,n**) and right (**c,f,i,l,o**) columns are extracted. The second column shows the profiles along the red line, which corresponds to a flight line, and the third column shows profiles along the yellow line (along flow). The solid black line shows the surface elevation along the transect, the dashed black line is sea level, the solid blue line is the bed elevation from BedMachine (with the associated uncertainty in light blue) and the green line is the bed topography from Bedmap2 (with the associated uncertainty in light green). The black dots and black error bars in the panels of the second column show the radar-derived bed elevation and associated uncertainty, respectively.

upstream of the present-day grounding line will prevent the glacier from rapid retreat into the deep Wilkes subglacial basin (red arrow, Fig. 2e). Subglacial ridges such as this one were not apparent in previous mappings but are robust features of our inversion that imply that such sectors have a low risk of collapse in decades to come (for example, Fig. 3f and Supplementary Figs. 18–21).

Along George V Land (Fig. 2f), the bed of Ninnis Glacier displays strong glacial lineations, tens of kilometres long, probably resulting from bedrock erosion over multiple glacial cycles. The bed is flatter in this region; that is, the flow of Ninnis is not as strongly topographically controlled as at Byrd Glacier, but is more similar to Thwaites. We find a 10 km-wide valley beneath the fast-flowing portion of the glacier that extends 70 km upstream and is thus more prominent and extensive than in Bedmap2 (Fig. 2f and Supplementary Fig. 27). This glacier has been relatively stable over past decades, but recently lost a large part of its floating tongue[15], and its bed topography suggests susceptibility to marine ice sheet instability[24] (MISI) that has not been highlighted previously. Conversely, further west in Wilkes Land (Fig. 2g and Supplementary Figs. 32 and 33), we find that Totten Glacier (3.9 m SLE, 65 Gt per year) and Moscow University Ice Shelf flow over a mostly prograde bed for 50 km upstream of the current grounding line at Totten and for 60 km at Moscow. Despite the significant thinning signal observed on Totten Glacier, evidence of a slow grounding line retreat[25], the presence of relatively warm water in front of the glacier[26] and high rates of ice shelf melt, we find that the bed topography is likely to limit any widespread MISI in that sector, until the grounding line retreats past the prograde slope areas.

Further west, Denman Glacier flows through a deep canyon more than ~3,500 m below sea level. The full depth of the bed was not resolved even in the most recent radar field campaigns (Fig. 3h) due to its deep entrenchment and the presence of a rough and broken-up ice surface[3,5] (Supplementary Fig. 35). BedMachine reveals that the bed beneath this ice stream is the deepest continental point on Earth. Close to the grounding line, the bed slope is gentle and slightly retrograde, which could lead to instability if the grounding line were to retreat inland, making this sector very vulnerable in East Antarctica, with a potential 1.5 m sea level rise.

On Mellor Glacier, upstream of Amery Ice Shelf, we find a 3 km-deep bed depression (Figs. 2i and 3j) that is inconsistent with previous radar data that indicated a bed only 1,000 m below sea level, and which also yielded ice fluxes that were much too low to balance upstream accumulation. We conclude that the radar data have been systematically misinterpreted in that region, probably due to side reflections (Fig. 3k,l and Supplementary Fig. 37). MC requires ice to be more than 1 km thicker at that location, which is quite plausible because this is a zone of convergence of three glaciers (Lambert, Mellor and Fisher) constrained by mountain ranges. The valleys are mostly prograde and the basin upstream rises rapidly above sea level except along the East Lambert Rift, suggesting that this sector has low potential for MISI in the near future.

Bed topography further west, stretching from Enderby to Queen Maud Land, is locally retrograde only for a few tens of kilometres (Supplementary Fig. 60) and is therefore not as vulnerable to MISI as other regions. In the Baudouin sector, West Ragnhild Ice Stream flows on a prograde submarine valley that extends 80 km further inland[27] than in Bedmap2, but eventually rises above sea level (Fig. 2j). Conversely, further west along Coats Land, several major ice streams feeding the Ronne–Filchner Ice Shelf stand on strongly retrograde bed slopes from 100 to 600 km farther upstream than in Bedmap2: Slessor (2.9 m SLE), Recovery (6.2 m SLE), Support Force and Academy (2.5 m SLE). Recovery (Fig. 2k) is 800 m deeper than previously thought (Fig. 3o and Supplementary Fig. 46). This region is a major point of vulnerability in East Antarctica.

At the southeastern tip of the Antarctic Peninsula, we report a well-defined valley that coincides with Evans Ice Stream and four tributaries feeding the main ice stream (Fig. 3l). This sector is an example of selective linear erosion characterized by more rapid basal incision by fast-flowing, warm-based ice relative to the surrounding slower, cold-based ice. Some tributaries flow in troughs more than 2 km below sea level that drain ice from a predominantly submarine basin.

Among the limitations of our compilation, we note a lack of ocean bathymetry on the continental shelf and beneath ice shelves, which remains a problem over vast portions of the coast of Antarctica. Multibeam echo sounding data, gravity data, seismic data and sea floor depth from robotic devices will be essential to improve bathymetry mapping in this part of Antarctica, which is critical for ice/ocean interactions and for ice sheet mass balance[28]. To improve the mapping of fast-flowing regions, we recommend flight tracks perpendicular to the flow direction to maximize constraints on ice flux, especially upstream of Academy and Support Force glaciers, along Stancomb-Wills, Gould Coast near the Ross Ice Shelf, and Wilhem II Coast between Denman and Lambert glaciers.

Implications for ice sheet vulnerability

The new bed topography highlights regions of higher vulnerability in West Antarctica and regions of low risk in the Ross Sea sector, along the Transantarctic Mountains. Glaciers spanning from George V Land to Dibble Glacier in Terre Adélie and Wilkes Land are, in contrast, located at the mouth of deep submarine basins with retrograde slopes, and hence risk zones for MISI. In Wilkes Land, Totten Glacier and Moscow University Ice Shelf would have to retreat ~50 km inland before reaching a zone of retrograde bed, but Denman Glacier stands at the edge of a deep trough that makes it vulnerable. Further west, the glaciers in Enderby and Queen Maud Land flow over prograde bed slope, except along a narrow coastal margin, and the drainage basins are mostly above sea level, hence more protected from MISI. Conversely, the glaciers feeding the eastern side of the Filchner Ice Shelf have retrograde slopes over vast portions of their basin and hence are prone to MISI. It will be essential to refine these results with more precise observations in the future to better inform ice sheet numerical models, but the new product has already brought major changes that call into question prior modelling using older maps. The revised bed topography will enable more robust ice sheet numerical modelling and improved projections of the contribution of Antarctica to sea level rise.

Online content

Any methods, additional references, Nature Research reporting summaries, source data, extended data, supplementary information, acknowledgements, peer review information; details of author contributions and competing interests; and statements of data and code availability are available at https://doi.org/10.1038/s41561-019-0510-8.

References

1. Evans, S. & Robin, Gd. Q. Glacier depth-sounding from air. *Nature* **210**, 883–885 (1966).
2. Pritchard, H. D. Bedgap: where next for Antarctic subglacial mapping? *Antarct. Sci.* **26**, 742–757 (2014).
3. Holt, J. W., Peters, M. E., Kempf, S. D., Morse, D. L. & Blankenship, D. D. Echo source discrimination in single-pass airborne radar sounding data from the dry valleys, Antarctica: implications for orbital sounding of Mars. *J. Geophys. Res.* **111**, E06S24 (2006).
4. Jezek, K., Wu, X., Paden, J. & Leuschen, C. Radar mapping of Isunnguata Sermia, Greenland. *J. Glaciol.* **59**, 1135–1146 (2013).
5. Fretwell, P. et al. Bedmap2: improved ice bed, surface and thickness datasets for Antarctica. *Cryosphere* **7**, 375–393 (2013).
6. Durand, G., Gagliardini, O., Favier, L., Zwinger, T. & le Meur, E. Impact of bedrock description on modeling ice sheet dynamics. *Geophys. Res. Lett.* **38**, L20501 (2011).

7. Morlighem, M. et al. A mass conservation approach for mapping glacier ice thickness. *Geophys. Res. Lett.* **38**, L19503 (2011).

8. Seroussi, H. et al. Ice flux divergence anomalies on 79 north glacier, Greenland. *Geophys. Res. Lett.* **38**, L09501 (2011).

9. Morlighem, M., Rignot, E., Mouginot, J., Seroussi, H. & Larour, E. Deeply incised submarine glacial valleys beneath the Greenland ice sheet. *Nat. Geosci.* **7**, 418–422 (2014).

10. Morlighem, M. et al. Bedmachine v3: complete bed topography and ocean bathymetry mapping of Greenland from multi-beam echo sounding combined with mass conservation. *Geophys. Res. Lett.* **44**, 11051–11061 (2017).

11. Rignot, E., Velicogna, I., van den Broeke, M. R., Monaghan, A. & Lenaerts, J. Acceleration of the contribution of the Greenland and Antarctic ice sheets to sea level rise. *Geophys. Res. Lett.* **38**, L05503 (2011).

12. Mouginot, J., Rignot, E., Scheuchl, B. & Millan, R. Comprehensive annual ice sheet velocity mapping using Landsat-8, Sentinel-1 and RADARSAT-2 data. *Remote Sens.* **9**, 364 (2017).

13. van Wessem, J. M. et al. Modelling the climate and surface mass balance of polar ice sheets using RACMO2: part 2: Antarctica (1979–2016). *Cryosphere* **12**, 1479–1498 (2018).

14. Howat, I. M., Porter, C., Smith, B. E., Noh, M.-J. & Morin, P. The reference elevation model of Antarctica. *Cryosphere* **13**, 665–674 (2019).

15. Rignot, E. et al. Four decades of Antarctic ice sheet mass balance from 1979–2017. *Proc. Natl Acad. Sci. USA* **116**, 1095–1103 (2019).

16. Bingham, R. G. et al. Diverse landscapes beneath Pine Island Glacier influence ice flow. *Nat. Commun.* **8**, 1618 (2017).

17. Rignot, E., Mouginot, J., Morlighem, M., Seroussi, H. & Scheuchl, B. Widespread, rapid grounding line retreat of Pine Island, Thwaites, Smith and Kohler glaciers, West Antarctica from 1992 to 2011. *Geophys. Res. Lett.* **41**, 3502–3509 (2014).

18. Joughin, I., Smith, B. E. & Medley, B. Marine ice sheet collapse potentially underway for the Thwaites Glacier Basin, West Antarctica. *Science* **344**, 735–738 (2014).

19. Seroussi, H. et al. Continued retreat of Thwaites Glacier, West Antarctica, controlled by bed topography and ocean circulation. *Geophys. Res. Lett.* **44**, 6191–6199 (2017).

20. Yu, H., Rignot, E., Seroussi, H. & Morlighem, M. Retreat of Thwaites Glacier, West Antarctica, over the next 100 years using various ice flow models, ice shelf melt scenarios and basal friction laws. *Cryosphere* **12**, 3861–3876 (2018).

21. Nias, I. J., Cornford, S. L. & Payne, A. J. New mass-conserving bedrock topography for Pine Island Glacier impacts simulated decadal rates of mass loss. *Geophys. Res. Lett.* **45**, 3173–3181 (2018).

22. Sugden, D. E. & John, B. S. *Glaciers and Landscape: A Geomorphological Approach* (Edward Arnold, 1976).

23. Jamieson, S. S. et al. The glacial geomorphology of the Antarctic ice sheet bed. *Antarct. Sci.* **26**, 724–741 (2014).

24. Weertman, J. Stability of the junction of an ice sheet and an ice shelf. *J. Glaciol.* **13**, 3–11 (1974).

25. Li, X., Rignot, E., Morlighem, M., Mouginot, J. & Scheuchl, B. Grounding line retreat of Totten Glacier, East Antarctica, 1996 to 2013. *Geophys. Res. Lett.* **42**, 8049–8056 (2015).

26. Rintoul, S. R. et al. Ocean heat drives rapid basal melt of the Totten Ice Shelf. *Sci. Adv.* **2**, e1601610 (2016).

27. Eagles, G. et al. Erosion at extended continental margins: insights from new aerogeophysical data in eastern Dronning Maud Land. *Gondwana Res.* **63**, 105–116 (2018).

28. Millan, R., Rignot, E., Bernier, V., Morlighem, M. & Dutrieux, P. Bathymetry of the Amundsen Sea Embayment sector of West Antarctica from operation icebridge gravity and other data. *Geophys. Res. Lett.* **44**, 1360–1368 (2017).

Methods

The MC method[7,29] yields ice thickness and bed topography compatible with ice sheet numerical models, resolves the uncertainties of previous interpretation of radar echoes, and ensures that grounding line fluxes are compatible with snowfall accumulation and thinning rates in the interior, without assuming a steady state. We use radar-derived thickness data from multiple sources, with a vertical precision of ~30 m, ice velocity measurements derived from satellite radar data posted at 150 m, with errors of 10 m per year in speed and 1.5° in flow direction[11], the REMA digital elevation model[14], gravity-derived bathymetry[28,30,31], seismic bathymetry[32] and IBCSO data[33], and surface mass balance[13] averaged for the years 1961–1990 with a 7% accuracy. The algorithm neglects ice motion by internal shear, which is a good approximation[7,29] for fast-flowing glaciers (>50 m per year). The optimization procedure is not applied in slow-moving sectors, where we use a streamline diffusion. For floating ice shelves, we rely on hydrostatic equilibrium with a calibrated firn depth correction so the inferred ice thickness is consistent with available ice thickness data. More technical details and error analyses are provided in the Supplementary Information.

Data availability

BedMachine Antarctica is publicly available at the NSIDC, Boulder, CO, as a MEaSUREs-3 product (http://nsidc.org/data/nsidc-0756).

Code availability

The algorithms used to generate the bed topography are included in the open-source Ice Sheet System Model (https://issm.jpl.nasa.gov).

References

29. Morlighem, M. et al. High-resolution bed topography mapping of Russell Glacier, Greenland, inferred from operation icebridge data. *J. Glaciol.* **59**, 1015–1023 (2013).

30. Greenbaum, J. S. et al. Ocean access to a cavity beneath Totten Glacier in East Antarctica. *Nat. Geosci.* **8**, 294–298 (2015).

31. Tinto, K. J. et al. Ross Ice Shelf response to climate driven by the tectonic imprint on seafloor bathymetry. *Nat. Geosci.* **12**, 441–449 (2019).

32. Rosier, S. H. R. et al. A new bathymetry for the southeastern Filchner–Ronne Ice Shelf: implications for modern oceanographic processes and glacial history. *J. Geophys. Res. Oceans* **123**, 4610–4623 (2018).

33. Arndt, J. E. et al. The International Bathymetric Chart of the Southern Ocean (IBCSO) version 1.0: a new bathymetric compilation covering circum-Antarctic waters. *Geophys. Res. Lett.* **40**, 3111–3117 (2013).

Author contributions

M.M. developed the algorithm and led the calculations. H.S. assisted in implementing the algorithm. M.M. and E.R. wrote the first draft of the manuscript. All authors contributed data and to the writing of the Article.

Competing interests

The authors declare no competing interests.

Additional information

Supplementary information is available for this paper at https://doi.org/10.1038/s41561-019-0510-8.

Correspondence and requests for materials should be addressed to M.M.

Peer review information Primary Handling Editor(s): Heike Langenberg.

Reprints and permissions information is available at www.nature.com/reprints.